

Electronic Supplementary Information (ESI)

Graphene-coated hybrid electrocatalysts derived from bimetallic metal-organic framework for efficient hydrogen generation

Xiao Li,^a Liu Yang,^a Tan Su,^{*b} Xinlong Wang,^a Chunyi Sun,^{*a} and Zhongmin Su^{*a}

^a*Institute of Functional Material Chemistry, Local United Engineering Lab for Power Battery,*

Northeast Normal University, Changchun, 130024 Jilin, People's Republic of China.

^b*Institute of Theoretical Chemistry, Jilin University, Changchun 130021, P. R. China.*

*E-mail: zmsu@nenu.edu.cn

Table of Contents

1. Crystal structure and physical characterization of **NiMo-MOF**
2. Physical characterization of **NiMo₂C@C**
3. Additional electrochemical experiments of **NiMo₂C@C**
4. Comparison of HER parameters of different non-Pt catalysts.

1. Crystal structure and physical characterization of **NiMo-MOF**

1.1 X-ray Crystallographic Analysis

X-ray single crystal data collection of **NiMo-MOF** was obtained on a Bruker SMART APEX II CCD diffractometer equipped with a graphite monochromator using Mo-K α radiation ($\lambda = 0.71073 \text{ \AA}$) at 293 K. A multiscan technique was used to perform adsorption corrections. All the structures were solved using direct methods and refined using the full-matrix least-squares method on F² with anisotropic thermal parameters for all non-hydrogen atoms using the SHELXL-97 program.¹ All hydrogen atoms were located in calculated positions and refined isotropically. In the **NiMo-MOF**, the disordered atoms O1A and O1B, O2A and O2B were split over two sites with occupancy of 0.5 and were anisotropically refined. In the **NiMo-MOF**, free water molecules were highly disordered, and we failed to locate and refine the solvent peaks. Then, we used the SQUEEZE routine of PLATON to remove the diffused electron densities resulting from the residual solvent molecules and further refined using the data generated.² The final formula of **NiMo-MOF** were determined by the combination of elemental analysis, TGA data and the SQUEEZE results. The crystallographic data for **NiMo-MOF** is listed in Table 1. Moreover, the selected bonds distances and bond angles are summarized in Table 2. In addition, crystallographic data of **NiMo-MOF** have been deposited in Cambridge Crystallographic Data Center as supplementary publication with CCDC number: 1515194.

Reference:

- (1) SHELXS-97, Sheldrick, G. M. *Acta Crystallogr. Sect. A: Found. Crystallogr.* **2008**, *64*, 112-122.
- (2) Spek, A. L. *Acta Crystallogr. Sect. D: Biol. Crystallogr.* **2009**, *65*, 148-155.

Table 1. Crystallographic Data for NiMo-MOF.

Compound	NiMo-MOF
Chemical formula	C ₂₆ H ₂₉ NiMoN ₄ O _{4.50}
Formula weight	624.18
Crystal system	Triclinic
Space group	<i>P-1</i>
<i>a</i> (Å)	12.673(2)
<i>b</i> (Å)	12.7426(19)
<i>c</i> (Å)	13.598(2)
α (°)	115.976(2)
β (°)	105.206(3)
γ (°)	102.326(3)
V (Å ³)	1763.3(5)
Temperature (K)	293(2)
<i>Z</i>	2
<i>D</i> _{calcd} (g · cm ⁻³)	1.176
GOF on <i>F</i> ²	0.858
no. of unique data	6437
no. of params refined	346
<i>R</i> _I [<i>I</i> > 2σ(<i>I</i>)] ^a	0.0503
w <i>R</i> ₂ [<i>I</i> > 2σ(<i>I</i>)] ^b	0.1219
<i>R</i> ₁ ^a (all data)	0.0895
w <i>R</i> ₂ ^b (all data)	0.1375
<i>R</i> _{int}	0.0436

^a $R_1 = \sum |F_0| - |F_c| / \sum |F_0|$. ^b $wR_2 = [\sum w(F_0^2 - F_c^2)^2 / \sum w(F_0^2)^2]^{1/2}$

Table 2. Selected Bonds Lengths (Å) and Angles (°) for compounds NiMo-MOF

Compound NiMo-MOF			
Ni(1)-O(4)#1	2.064(3)	Ni(2)-N(4)#4	2.137(4)
Ni(1)-O(4)	2.064(3)	Ni(2)-N(2)#5	2.153(4)
Ni(1)-N(3)	2.113(4)	Ni(2)-N(2)#6	2.153(4)
Ni(1)-N(3)#1	2.113(4)	Mo(1)-O(1)	1.650(14)
Ni(1)-N(1)	2.136(4)	Mo(1)-O(2)	1.681(15)
Ni(1)-N(1)#1	2.136(4)	Mo(1)-O(3)	1.740(3)
Ni(2)-O(3)	2.059(3)	Mo(1)-O(4)	1.757(3)
Ni(2)-O(3)#2	2.059(3)	Mo(1)-O(2A)	1.827(17)
Ni(2)-N(4)#3	2.137(4)	Mo(1)-O(1A)	1.863(13)
O(4)#1-Ni(1)-O(4)	180.0(2)	O(3)#2-Ni(2)-N(4)#4	89.79(15)
O(4)#1-Ni(1)-N(3)	89.96(14)	N(4)#3-Ni(2)-N(4)#4	180.0(2)
O(4)-Ni(1)-N(3)	90.04(14)	O(3)-Ni(2)-N(2)#5	89.57(14)
O(4)#1-Ni(1)-N(3)#1	90.04(14)	O(3)#2-Ni(2)-N(2)#5	90.43(14)
O(4)-Ni(1)-N(3)#1	89.96(14)	N(4)#3-Ni(2)-N(2)#5	87.73(16)
N(3)-Ni(1)-N(3)#1	180.0(3)	N(4)#4-Ni(2)-N(2)#5	92.27(16)
O(4)#1-Ni(1)-N(1)	89.24(14)	O(3)-Ni(2)-N(2)#6	90.43(14)
O(4)-Ni(1)-N(1)	90.76(14)	O(3)#2-Ni(2)-N(2)#6	89.57(14)
N(3)-Ni(1)-N(1)	93.15(16)	N(4)#3-Ni(2)-N(2)#6	92.27(16)
N(3)#1-Ni(1)-N(1)	86.85(16)	N(4)#4-Ni(2)-N(2)#6	87.73(16)
O(4)#1-Ni(1)-N(1)#1	90.76(14)	N(2)#5-Ni(2)-N(2)#6	180.0(2)
O(4)-Ni(1)-N(1)#1	89.24(14)	O(1)-Mo(1)-O(2)	88.3(6)
N(3)-Ni(1)-N(1)#1	86.86(16)	O(1)-Mo(1)-O(3)	112.6(6)
N(3)#1-Ni(1)-N(1)#1	93.15(16)	O(2)-Mo(1)-O(3)	115.0(6)
N(1)-Ni(1)-N(1)#1	180	O(1)-Mo(1)-O(4)	115.5(6)
O(3)-Ni(2)-O(3)#2	180	O(2)-Mo(1)-O(4)	113.3(6)
O(3)-Ni(2)-N(4)#3	89.79(15)	O(3)-Mo(1)-O(4)	110.72(15)
O(3)#2-Ni(2)-N(4)#3	90.21(15)	O(1)-Mo(1)-O(2A)	108.0(6)
O(3)-Ni(2)-N(4)#4	90.21(15)	O(2A)-Mo(1)-O(1A)	128.0(5)
O(2)-Mo(1)-O(2A)	19.8(6)	O(2)-Mo(1)-O(2A)	19.8(6)
O(3)-Mo(1)-O(2A)	103.9(6)	O(3)-Mo(1)-O(2A)	103.9(6)
O(4)-Mo(1)-O(2A)	105.2(5)	O(4)-Mo(1)-O(2A)	105.2(5)

Symmetry codes: for compound **NiMo-MOF**: #1 -x + 1, -y + 1, -z + 2; #2 -x + 1, -y + 2, -z + 2; #3 -x + 1, -y + 1, -z + 1; #4 x, y + 1, z + 1; #5 x + 1, y + 1, z; #6 -x, -y + 1, -z + 2.

1.2 Structure of compound NiMo-MOF.

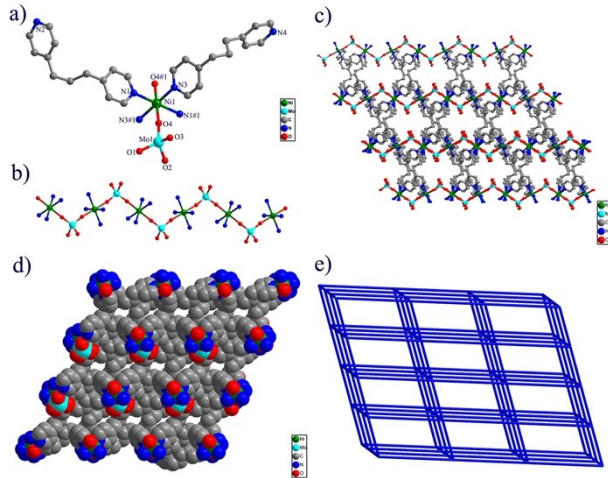


Fig. S1 (a) Ni(II) coordination environments of **NiMo-MOF**. Symmetry codes: (#1) $1 -x + 1, -y + 1, -z + 2$. (b) 1D chain of **NiMo-MOF**. (c) and (d) 3D framework of **NiMo-MOF** with 1D channels running along *a* and *b* axes. (e) 3D uninodal 6-connected net with a $\{4^{12} \cdot 6^3\}$ topology of **NiMo-MOF**. All hydrogen atoms are omitted for clarity.

X-ray determination has revealed that **NiMo-MOF** crystallized in the triclinic system with P-*I* space group. The asymmetric unit includes one Ni (II) ion, one Mo (VI) ion and two bpp ligands are shown in Figure S1a. Ni²⁺ adopts a hexacoordinated octahedral fashion geometry by connecting to two oxygen atoms and four nitrogen atoms from two bpp ligands. The average Ni-O and Ni-N distances are from 2.059 to 2.064(3) Å and from 2.113(4) to 2.153(4) Å, respectively. Mo⁶⁺ shows MoO₄ tetrahedron coordination configuration, and each molybdenum centre is coordinated with two bridging oxygen atoms (O_b) and two terminal oxygen atoms (O_t). The V-O_t distances of 1.650(14) and 1.681(15) Å are slightly shorter than the V-O_b distances of 1.740(3) and 1.757(3) Å. The Ni ions and adjacent Mo ions are connected through the bridging oxygen atoms to form a one dimensional chain, displayed in Fig S1b. Then, the one dimensional chains are further linked by bpp ligands to assemble into a 3D framework with 1D channels along *a*, *b* and *c* axes (Fig. S1c and S1d). Topologically, **NiMo-MOF** is a uninodal 6-connected net with the Schäfli symbol of $\{4^{12} \cdot 6^3\}$ as depicted in Figure. S3e.

1.3 Physical characterization of **NiMo-MOF**.

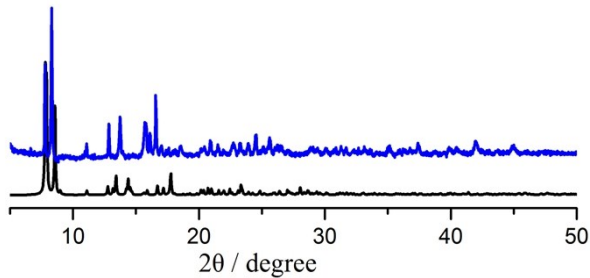


Fig. S2 Experimental (blue), simulated (black) PXRD patterns for compound **NiMo-MOF**.

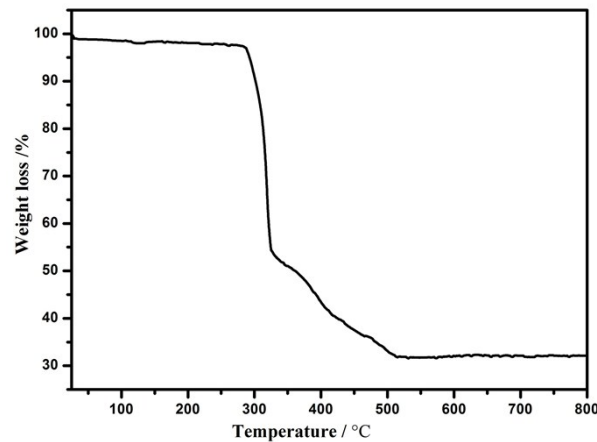


Fig. S3 The TGA curves for compound 1

To study the thermal stabilities of **NiMo-MOF**, the thermogravimetric analyses were carried out under N_2 atmosphere from room temperature to 800 °C with a heating rate of 10 °C min⁻¹. **NiMo-MOF** shows a slow weight loss of 1.56% before 280 °C, which corresponds to the loss of solvent water molecules (calculated 1.44%). Then with the increase of temperature, the framework collapsed and decomposed. The residues are NiO and MoO₃ (experimental: 32.28% and calculated 33.13%).

2. Physical characterization of **NiMo₂C@C**

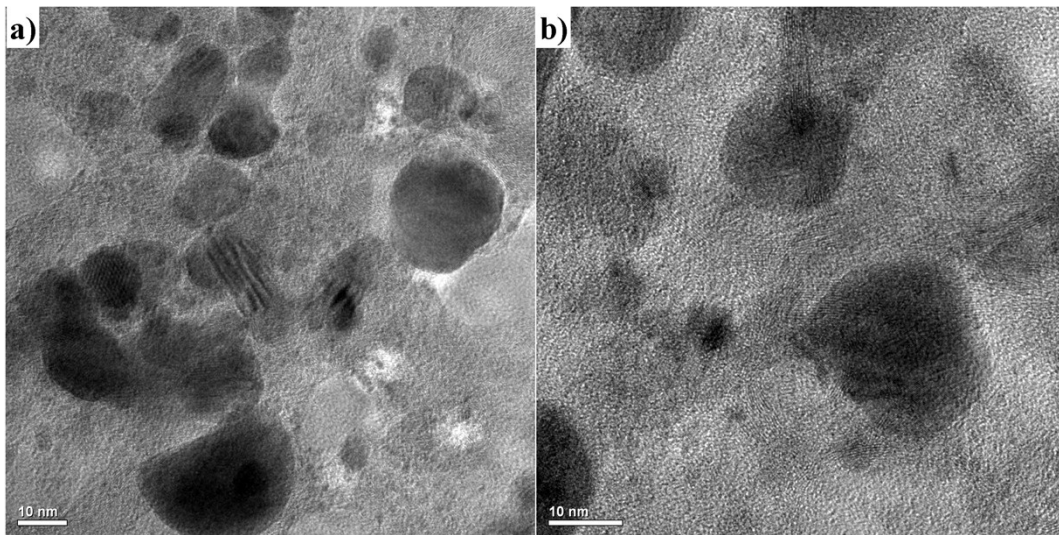


Fig. S4 (a) and (b) TEM images of NiMo₂C@C, displaying that Ni/Mo₂C nanoparticles are well coated with graphitized carbon layers.

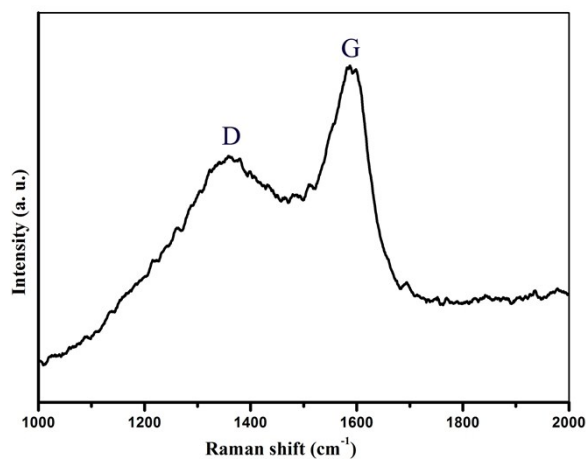


Fig. S5 Raman spectrum of NiMo₂C@C with $I_G/I_D = 1.2$, indicating the partial graphitization at 700 °C.

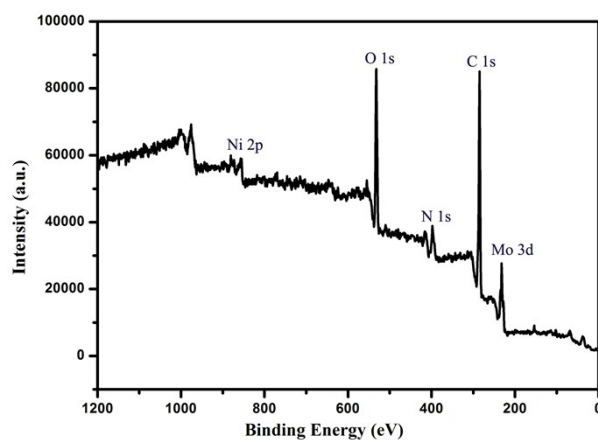


Fig. S6 X-ray photoelectron spectra of NiMo₂C@C.

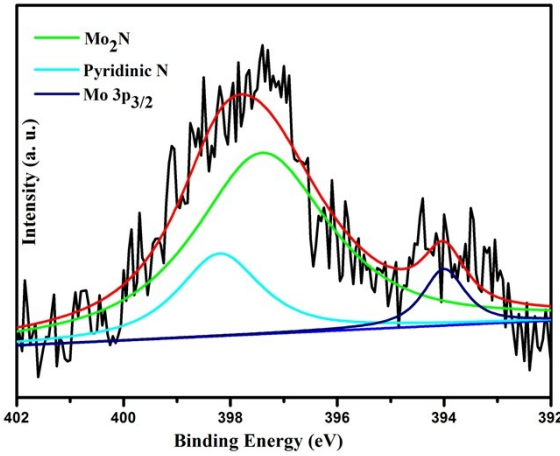


Fig. S7 The high resolution N 1s XPS of **NiMo₂C@C**.

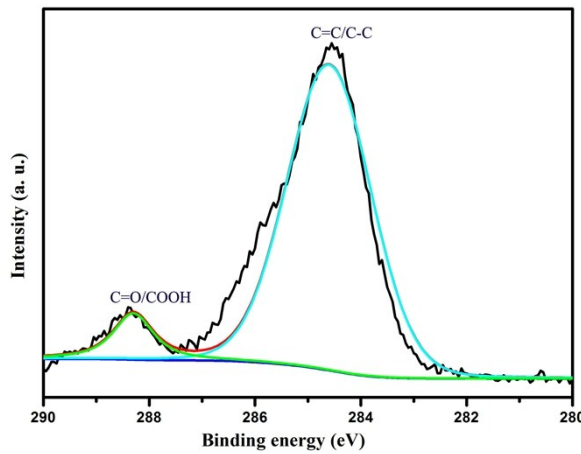


Fig. S8 The high resolution C 1s XPS of **NiMo₂C@C**. The position of the C 1s line ascribed to C=C/C-C is 284.6 eV, downshift by about 0.4 eV compared with GO (285.0 eV), which indicates the charge transfer between NiMo₂C and graphene.

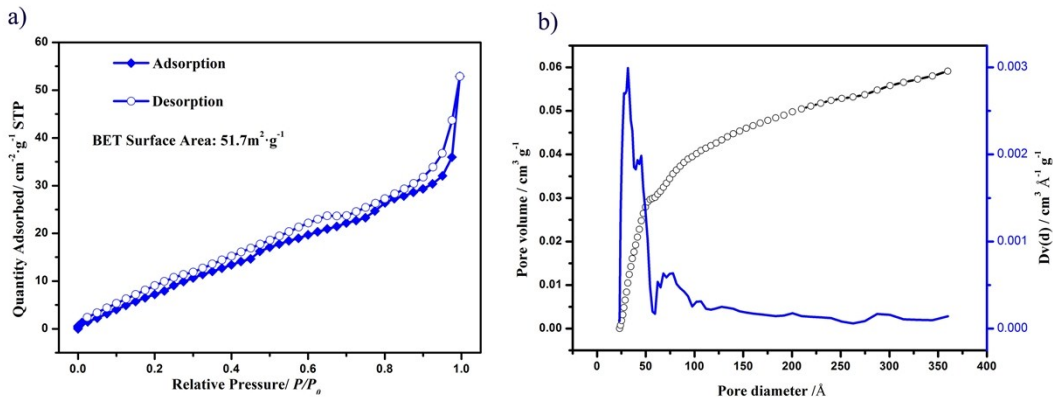


Fig. S9 (a) **N₂** adsorption-desorption isotherms. (b) The pore-size distribution of **NiMo₂C@C**.

3. Additional electrochemical experiment of **NiMo₂C@C**

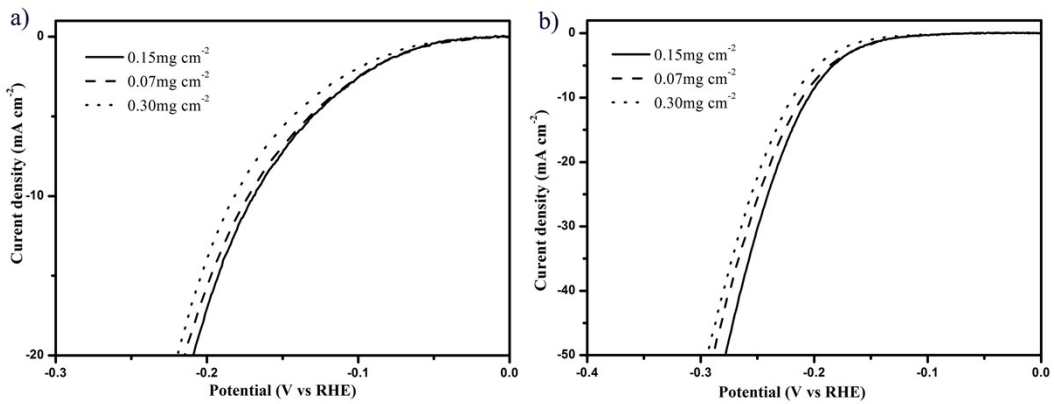


Fig. S10 (a) and (b) Polarization curves of **NiMo₂C@C** with different mass loadings on a glassy carbon electrode in 0.5M H₂SO₄ and 1M KOH.

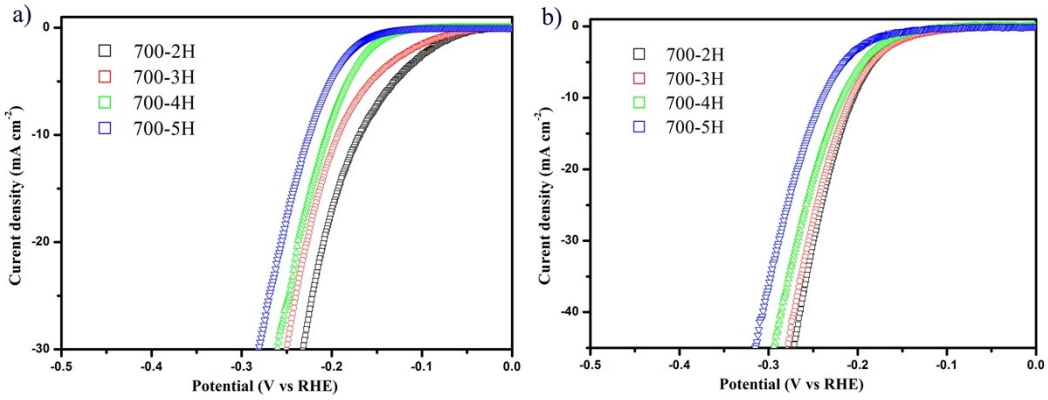


Fig.S11 (a) and (b) Polarization curves of **NiMo₂C@C** with different carburizing time at 700 °C on a glassy carbon electrode in 0.5M H₂SO₄ and 1M KOH.

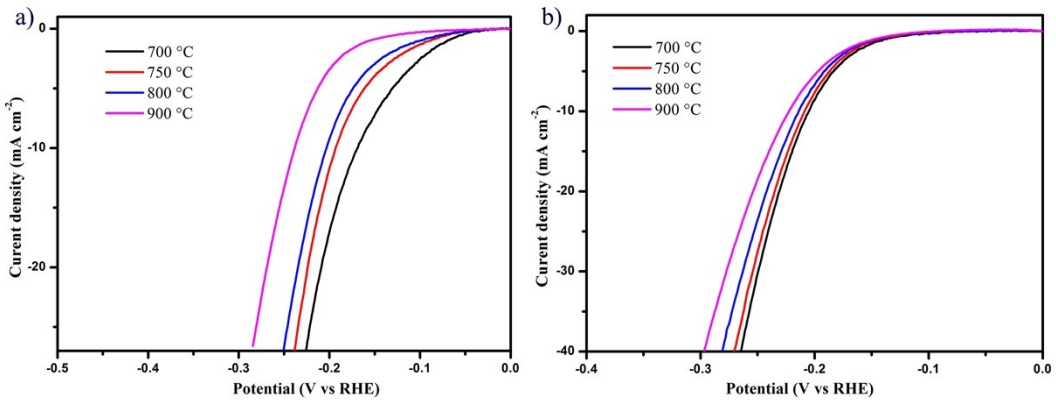


Fig.S12 (a) and (b) Polarization curves of **NiMo₂C@C** with different carburizing temperatures on a glassy carbon electrode in 0.5M H₂SO₄ and 1M KOH.

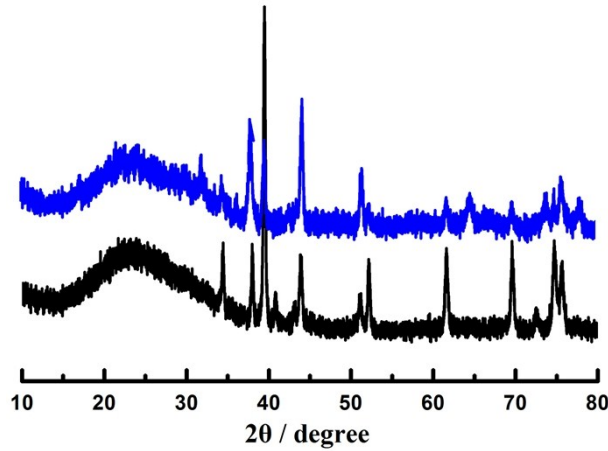


Fig. S13 PXRD curves of **NiMo₂C@C catalyst** (black) and **NiMo₂C@C catalyst of mixture** (blue).

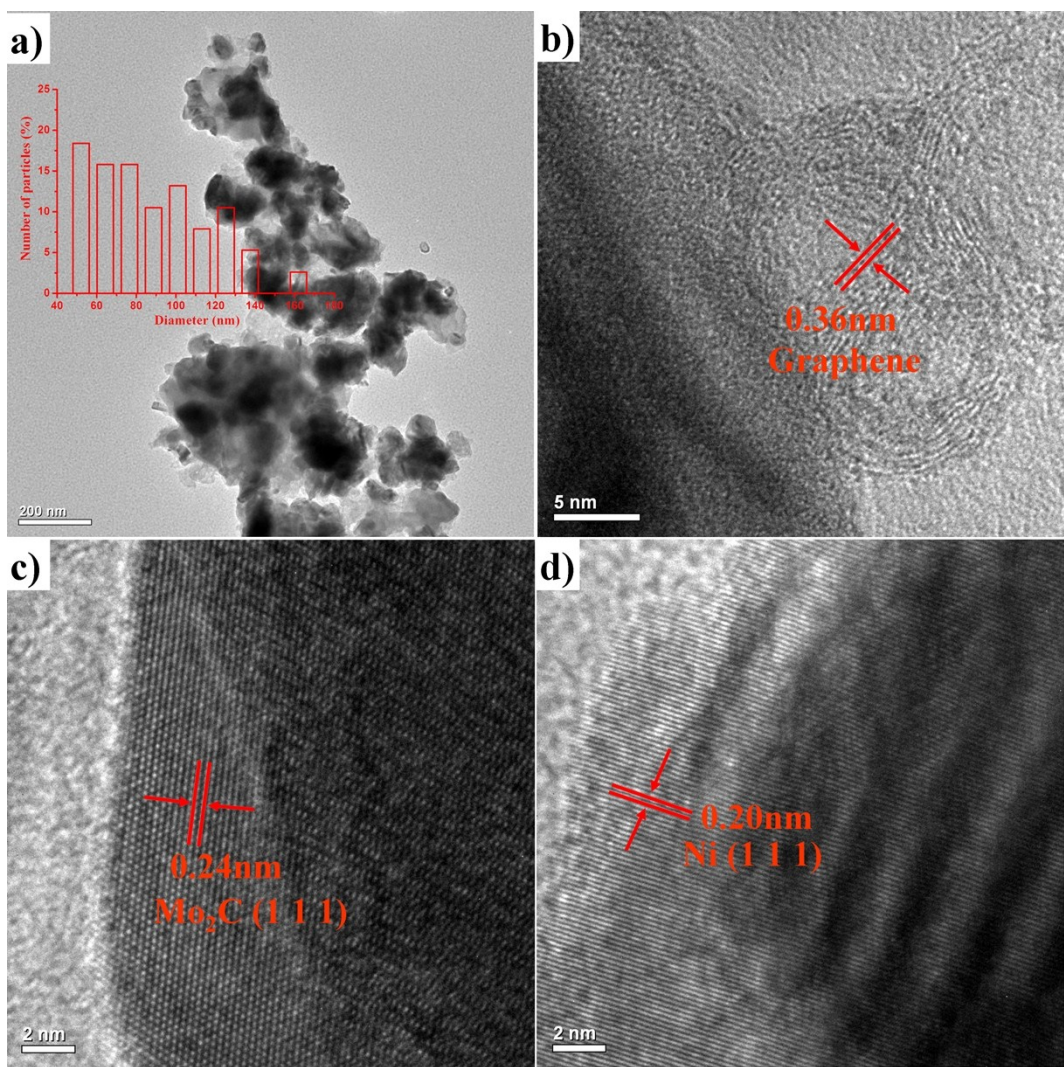


Fig. S14 (a) TEM image of **NiMo₂C@C (mixture)** (inset the particle size distribution of Ni/Mo₂C in **NiMo₂C@C (mixture)**), displaying Ni/Mo₂C nanoparticles possess a diameter range from 50nm to 160nm, which is much larger than the Ni/Mo₂C nanoparticles in **NiMo₂C@C catalyst**; (b-d) HRTEM images of **NiMo₂C@C (mixture)**. The d-spacing distance of multiple graphene layers, the lattice plane (111) of Mo₂C (JCPDS no. 15-0457) and Ni (JCPDS no. 04-0850) is about 0.36nm, 0.24nm and 0.20nm, respectively, which is well accordant with the **NiMo₂C@C catalyst**.

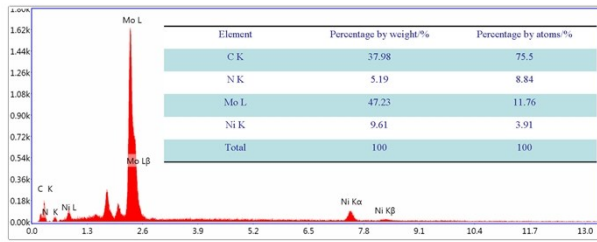


Fig. S15 The energy dispersive spectrum (EDS) of $\text{NiMo}_2\text{C}@\text{C}$ (mixture). The peaks corresponding to C, N, Mo and Ni elements are observed.

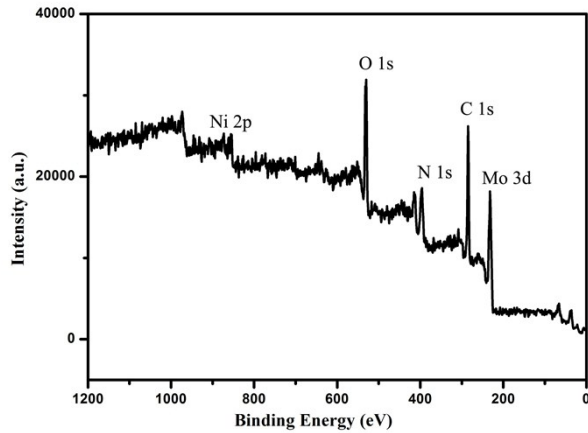


Fig. S16 X-ray photoelectron spectra of $\text{NiMo}_2\text{C}@\text{C}$ (mixture).

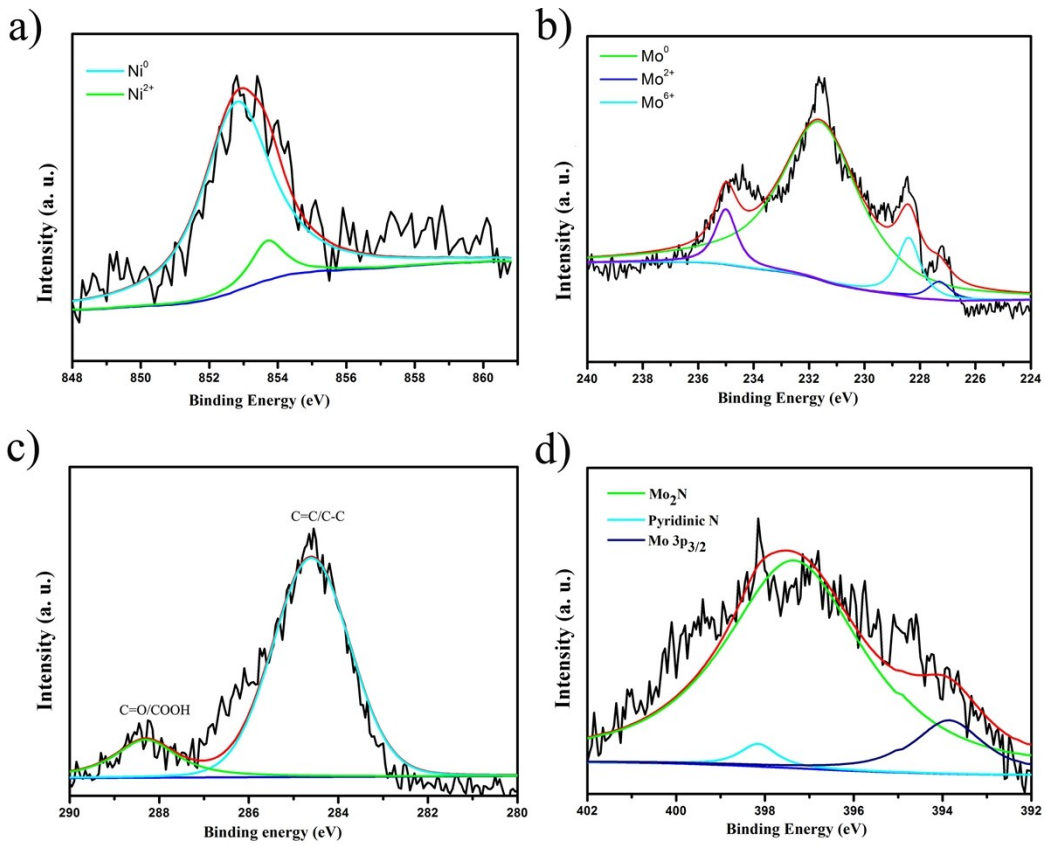


Fig. S17 (a) - (d) XPS spectra of Ni 2p peaks, Mo 3d peaks, C1s peaks and N 1s of **NiMo₂C@C** (mixture). The Ni 2p XPS spectrum of **NiMo₂C@C** (mixture) also displays the coexistence of Ni^0 (852.8 eV) and Ni^{2+} (853.7 eV). The Mo 3d XPS spectrum exhibits the existence of Mo^0 (227.3 eV), Mo^{2+} (228.4 eV) and Mo^{6+} (231.6 eV). The peak located at 284.6 eV of C 1s line is $\text{C}=\text{C/C-C}$. The peak located at 398.2 eV of N 1s XPS can be ascribed to pyridinic nitrogen derived from the bpp ligands. Therefore, the **NiMo₂C@C** (mixture) shows same binding state with **NiMo₂C@C**.

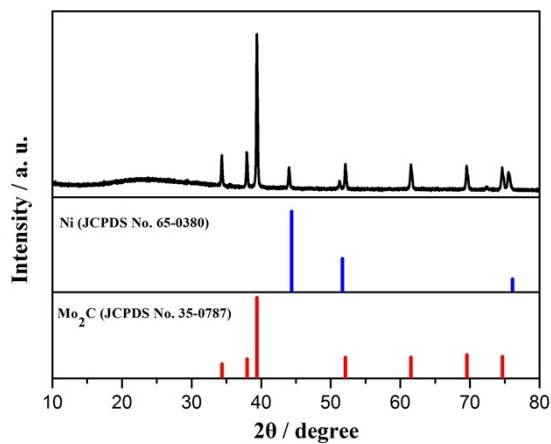


Fig. S18 PXRD curves of mixture with glucose.

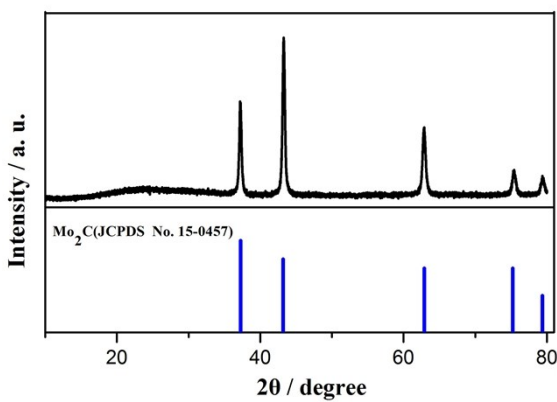


Fig. S19 PXRD curves of mixture with urea.

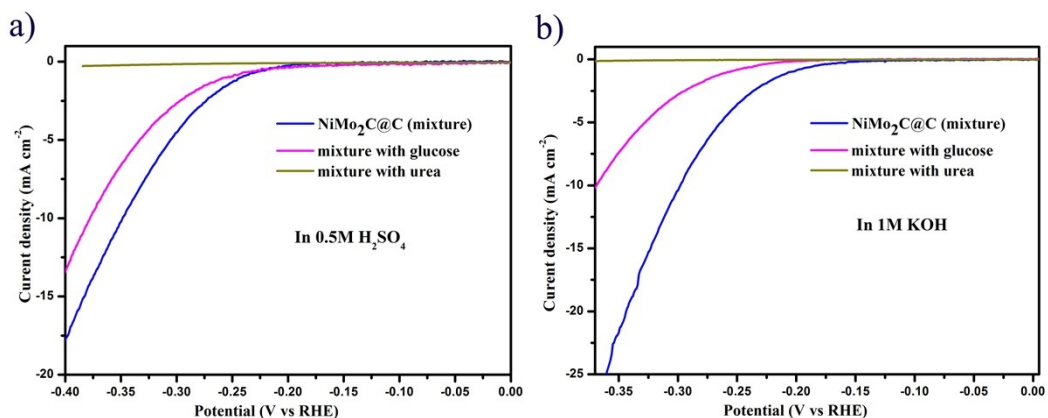


Fig. S20 (a) and (b) Polarization curves of **NiMo₂C@C** (mixture), mixture with glucose and mixture with urea on a glassy carbon electrode in 0.5M H₂SO₄ and 1M KOH.

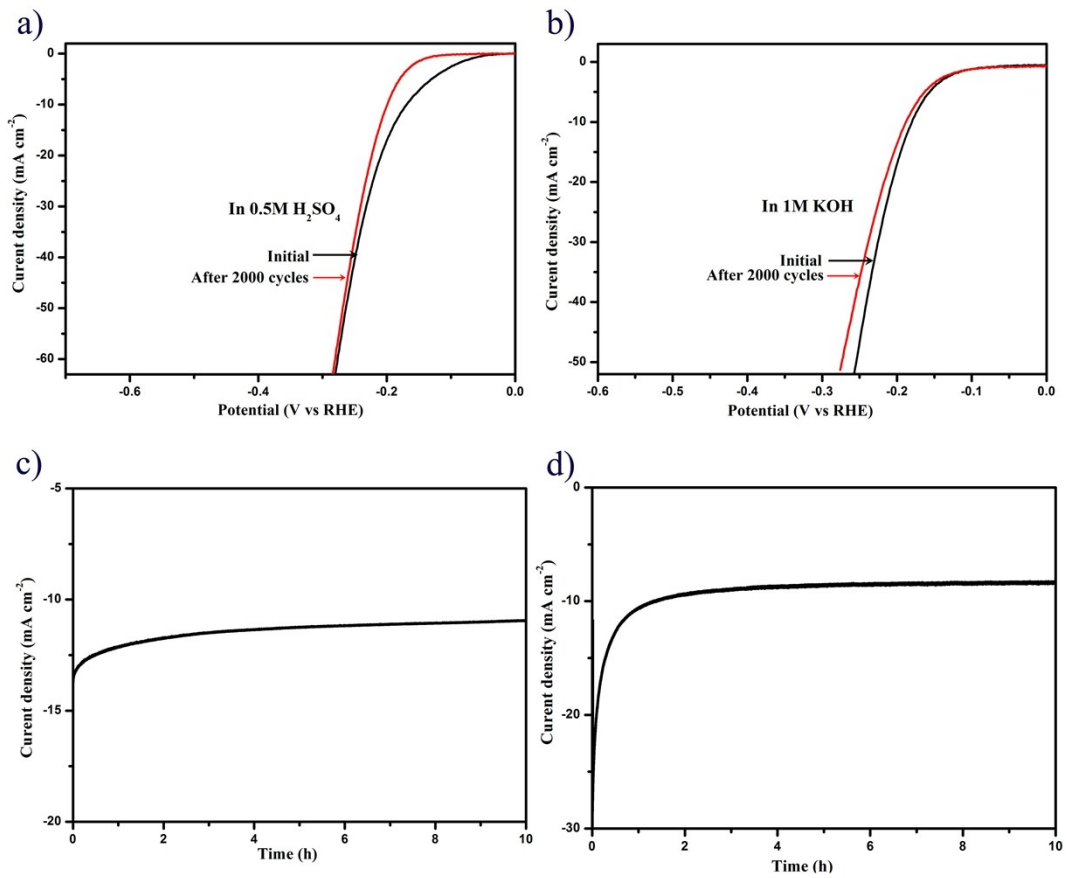


Fig. S21 (a) and (b) Polarization curves after continuous potential sweeps at 50 mV s^{-1} in $0.5\text{M H}_2\text{SO}_4$ and 1M KOH . (c) and (d) Time-dependent current density curves under $\eta = 180 \text{ mV}$ in $0.5\text{M H}_2\text{SO}_4$ and 1M KOH .

4. Comparison of HER parameters of different non-Pt catalysts.

Table S3 Comparison for HER activity in acidic solutions for **NiMo₂C@C** with other electrocatalysts.

Catalysts	Loading mass (mg cm ⁻²)	Current density (j , mA cm ⁻²)	η at corresponding j (mV)	Tafel slope (mV decade ⁻¹)	Ref.
NiMo₂C@C	0.15	10	169	100	This work
Mo ₂ C/CNT	2.0	10	152	55.2	S1
Mo ₂ C/CNT-graphene	0.65-0.67	10	130	58	S2
Co _{0.6} Mo _{1.4} N ₂	0.24	10	200	/	S3
MoS _x /graphene/Ni foam	5.01	10	141	42.8	S4
Mo _x C/Ni	—	10	~ 150	—	S5
NiMoN _x nanosheets	0.25	2	170	35.9	S6
Mo ₂ C-carbon nanocomposites	0.25	10	147	110-235	S7
Porous MoC _x nano-octahedrons	0.8	10	142	53	S8
MoO ₂ P _x /Mo	-	10	135	62	S9
Mo ₂ C and MoB microparticles	1.4-2.5	20	~225	55-56	S10

Table S4 Comparison for HER activity in basic solutions for **NiMo₂C@C** with other electrocatalysts.

Catalysts	Loading mass (mg cm ⁻²)	Current density (j , mA cm ⁻²)	η at correspondgding j (mV)	Tafel slope (mV decade ⁻¹)	Ref.
NiMo₂C@C	0.15	10	181	84	This work
Porous MoC _x nano-octahedrons	0.8	10	151	59	S8
Mo ₂ C and MoB microparticles	0.8-2.3	20	210-240	54-59	S10
Ni-Mo nanopowder	1	10	~80	-	S11
NiO/Ni-CNT	0.28	10	80	82	S12
NiMo ₂ C/NF	-	10	150	36.8	S13
Ni/Mo ₂ C-PC	0.5	10	179	101	S14
CoO _x @CN	0.12	10	232	115	S15
Mo ₂ C-NCNT	3	10	257	71	S16
Mo ₂ C	0.009	10	270	67	S17
MoB	2.3	10	~220	59	S18

Reference

- S1. W. F. Chen, C. H. Wang, K. Sasaki, N. Marinkovic, W. Xu, J. T. Muckerman, R. R. Adzic, *Energy Environ. Sci.*, **2013**, *6*, 943-951.
- S2. D. H. Youn, S. Han, J. Y. Kim, J. Y. Kim, H. Park, S. H. Choi, J. S. Lee, *ACS nano*, **2014**, *8*, 5164-5173.
- S3. B. Cao, G. M. Veith, J. C. Neuefeind, R. R. Adzic, P. G. Khalifah, *J. Am. Chem. Soc.*, **2013**, *135*, 19186-19192.
- S4. Y. H. Chang, C. T. Lin, T. Y. Chen, C. L. Hsu, Y. H. Lee, W. Zhang, L. J. Li, *Adv. Mater.*, **2013**, *25*, 756-760.
- S5. J. Zhang, X. Meng, J. Zhao, Z. Zhu, *ChemCatChem*, **2014**, *6*, 2059 – 2064.
- S6. W. F. Chen, K. Sasaki, C. Ma, A. I. Frenkel, N. Marinkovic, J. T. Muckerman, R. R. Adzic, *Angew. Chem. Int. Ed.*, **2012**, *51*, 6131-6135.
- S7. N. S. Alhajri, D. H. Anjum, K. Takanabe, *J. Mater. Chem. A.*, **2014**, *2*, 10548–10556.
- S8. H. B. Wu, B. Y. Xia, L. Yu, X. Y. Yu, X. W. Lou, *Nat. Commun.* **2015**, *6*, 6512-6519
- S9. X. Xie, R. Yu, N. Xue, A. B. Yousaf, H. Du, K. Liang, N. Jiang and A-W. Xu, *J. Mater. Chem. A*, **2016**, *4*, 1647–1652
- S10. H. Vrubel, X.L. Hu, *Angew. Chem. Int. Ed.*, **2012**, *124*, 12875-12878.
- S11. J. R. McKone, B. F. Sadtler, C. A. Werlang, N. S. Lewis, H. B. Gray, *2012, ACS Catal.*, *3*, 166-169.
- S12. M. Gong, W. Zhou, M. C. Tsai, J. G. Zhou, M. Y. Guan, M. C. Lin, B. Zhang, Y.F. Hu, D.Y. Wang, J. Yang, S. J. Pennycook, B. J. Hwang, H. J. Dai, *2014, Nat. Commun.*, *5*.
- S13. K. Xiong, L. Li, L. Zhang, W. Ding, L. S. Peng, Y. Wang, Z. D. Wei, *J. Mater. Chem. A.*, **2015**, *3*, 1863-1867.
- S14. Z. Y. Yu, Y. Duan, M. R. Gao, C. C. Lang, Y. R. Zheng, S. H. Yu, *Chemical Science*. **2016**.
- S15. H. Y. Jin, J. Wang, D. F. Su, Z. Z. Wei, Z. F. Pang, Y. Wang, *J. Am. Chem. Soc.*, **2015**, *137*, 2688-2694.
- S16. K. Zhang, Y. Zhao, D. Y. Fu, Y. J. Chen, *J. Mater. Chem. A.*, **2015**, *3*, 5783-5788.
- S17. C. G. Morales-Guio, K. Thorwarth, B. Niesen, L. Liardet, J.Patscheider, C. Ballif, X.l. Hu *J. Am. Chem. Soc.*, **2015**, *137*, 7035-7038.
- S18. H. Vrubel, X.L. Hu, *Angew. Chem. Int. Ed.*, **2012**, *51*, 12703 –12706.